ARTICLES

Probing DNA−DNA Electrostatic Friction in Tight Superhelical DNA Plies

A. G. Cherstvy[†]

Institute of Solid State Research, IFF, Theorie-II, Forschungszentrum Jülich, D-52425 Jülich, Germany

Received: November 28, 2008; Revised Manuscript Received: January 22, 2009

We estimate theoretically the strength of DNA−DNA electrostatic friction forces emerging upon a slow drag of one DNA over another one in a close juxtaposition. For ideally helical DNA duplexes, this friction occurs due to correlations in electrostatic potential near the DNA surface. The latter originate from the intrinsic helicity of DNA phosphates and adsorbed cations on a scale of 3.4 nm. They produce positive−negative charge interlocking along the DNA−DNA contact. For realistic nonideally helical DNAs, where electrostatic potential barriers become decorrelated due to accumulation of mismatches in DNA structure, DNA−DNA frictional forces are strongly impeded. We discuss possibilities of probing the DNA−DNA intermolecular interactions in strongly confined DNA superhelical plies, as obtained in single-molecule experiments.

I. Introduction: DNA Ply Experiments

The latest progress in single-molecule manipulation techniques has allowed the measurement of several new characteristics of the DNA elastic response as well as some properties of DNA−DNA and DNA−protein interactions. Optical and magnetic trap techniques applied to DNA superhelical plies have allowed exertion of forces and torques onto DNA molecules in order to control axial proximity of DNAs in the ply, with a possibility of probing mutual forces between the molecules.

Dual Optical Trap. The four-trap optical tweezers technique constructed recently by the group of Wuite[1] has allowed monitoring forces emerging upon dragging of two interwound DNA molecules along each other. The general motivation was to track the DNA molecular details on the nanoscale and to probe possible effects of DNA helicity on forces acting between DNA double helices. Typical DNA−DNA separations in these setup were estimated as $2R \approx 50-100$ Å. Both in the presence of mono- and multivalent counterions (e.g., with 0.2 mM spermine^{4+}, the cations known to induce DNA−DNA attraction), for different scanning speeds of 200−2000 DNA base pairs (bp) per second, and for various tensions applied to DNA molecules, *no* substantial DNA−DNA friction has been detected in the measurements. Pulling forces to drag one DNA over the other of well below ∼1 pN were measured, for both a single and multiple DNA turns in the supercoil; see Figure 1.

On the other hand, in the presence of some restriction enzymes, which were bound to double-stranded DNA and thus presented an obstacle for a sliding of another duplex over it, quite considerable friction forces were measured. Namely, the pulling forces of ∼2 and 5 pN were detected correspondingly for protein binding to nonspecific and specific sites on DNA. Here, the experiments were done at a typical speed of ≈500 bp/s, with a spatial resolution of ∼120 DNA bp. Note however that no measurements of superhelix opening angle or helical pitch P of the ply were possible in these experiments.

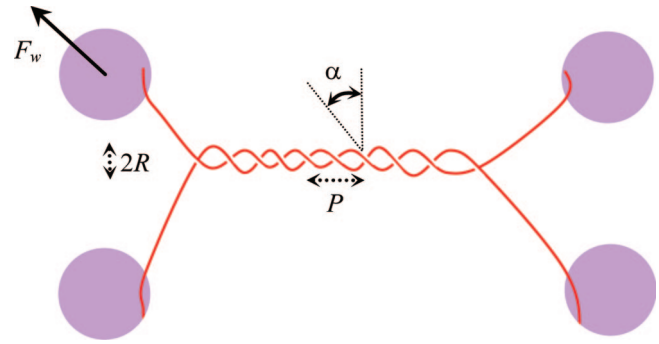

Figure 1. Schematics of DNA ply stretched by four beads in the dual trap optical tweezers apparatus.

Recently, the binding properties of DNA-associated proteins, H−NS, have been studied by the same technique.[2] These dimeric proteins interact nonspecifically with about one-pitch-long stretch of DNA, being capable of *bridging* two closely positioned parallel DNAs together. Both DNA shearing and DNA unzipping experiments were performed. The forces required to disrupt the protein−DNA complexes formed were shown to increase with the speed of motion of end beads, consistent with the explanation of increasing number of DNA−protein contacts to be disrupted per unit time. The disruption force for shearing was detected to be ∼25 pN at the speed of 22 nm/s, while for unzipping of complexes the forces of 2−7 pN at 22 nm/s and ∼10−30 pN at 88 nm/s are required. For the latter experiments, the complex disruption was shown to occur in a stepwise fashion, with step lengths being the multiples of DNA helical pitch, $H \approx 34$ Å, characterizing the spacings between H−NS bridges connecting two DNAs. Typically, the bridges are formed every two to six DNA helical repeats in these experiments. The forces required to shear two interwound DNAs are thus of a *frictional nature*, and they emerge due to mutual direct DNA−DNA and DNA−protein−DNA interactions in the ply. The current spatial resolution reported for the dual optical trap apparatus is ∼50 bp.

[†] E-mail: a.cherstvy@fz-juelich.de.

10.1021/jp810473m CCC: $40.75
Published on Web 03/30/2009

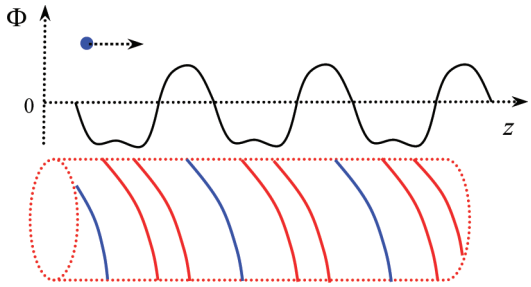

Figure 2. Schematic view of electrostatic potential barriers $\Phi(z) = e_0\phi(z)/(k_BT)$ near the DNA surface. Negative phosphate strands are shown in red; the density of counterions adsorbed in the DNA major groove is depicted in blue. The $\Phi(z)$ variations exceed unity in 2−5 Å proximity to the DNA surface.[6]

Magnetic Tweezers. Force−extension curves for a ply of two DNAs measured by magnetic tweezers apparatus by Charvin et al.[3] have revealed a small but repetitive difference for left- vs right-handed supercoiled DNA plies. That is, right-handed superhelices have revealed up to 10% larger extensions than left-handed ones.[4] The former can thus be braided stronger prior to a buckling transition into a tightly interwound state that takes place at a larger DNA supercoiling degree, σ. These differences in force−extension curves can indicate the effects of DNA molecular helicity on DNA winding properties and probably different DNA−DNA interactions in DNA plies of different spirality. Another possibility however is that the persistence length of left- and right-handed DNA plies is not the same, due to a different response of a ply to over- and under-winding.

The measured force−extension curves of DNA plies have been well reproduced by Monte Carlo simulations performed in this study with an effective, salt-dependent diameter of a DNA rod. The difference for left- vs right-handed plies has not been studied because simulations were based on interactions of uniformly charged rods that neglect DNA helicity. DNA braid diameter was shown to decrease with the force applied to the ply, consistently with predictions of statistical theory of DNA supercoils by Marko.[5] In this theory, for tight DNA braids the ply radius scales as $R \propto F^{-3/4}$ with the applied end force F.

The paper is organized as follows. First, we present the results of the theory of electrostatic interactions of DNA duplexes. Then, we calculate the magnitude of DNA−DNA frictional forces for ideal and nonideally helical DNAs. We show that the friction between two DNAs in a DNA ply can be caused entirely by helical distribution of DNA charges that creates a *periodic* DNA−DNA interaction potential with respect to the longitudinal shift δz of two DNAs in contact. Finally, we discuss the approximations used and summarize the results.

II. DNA Charge Compensation and DNA Electrostatic Potential

The energy to be paid to drag two interwound ideal DNA duplexes one over the other originates from electrostatic barriers in the proximity of the DNA helix. These barriers are experienced by charges in DNA neighboring and thus determine DNA−DNA electrostatic interaction. Particularly in solutions of multivalent cations, the electrostatic potential is negative near DNA phosphate strands and positive close to DNA grooves; see Figure 2. Positive charges in DNA grooves emerge due to adsorption of counterions from solution onto highly charged DNA. For many large multivalent cations this adsorption is known to occur mainly into the DNA major groove.

The adsorbed counterions neutralize a large fraction of charge of DNA phosphates, about 75−90%, depending upon the valence of cations and their chemical binding specificity. According to the Manning theory of counterion condensation onto highly charged thin, long polyelectrolytes,[7,8] the fraction of rod charge neutralized by adsorbed cations of valence z is

$$\theta \approx 1 - 1/(z\xi)$$

at low concentrations n_0 of electrolyte. Here, $\xi = l_B/b \approx 4.2$ is the DNA charge parameter, $b = 1.7$Å is the separation of DNA negative charges as calculated along the axis, and $l_B = e_0^2/(\varepsilon k_BT) \approx 7$ Å is the Bjerrum length in water with a dielectric constant of $\varepsilon \approx 80$. The model of a thin rod was shown to work quite well for description of long double helical DNAs. There exist many modifications of this theory for polyelectrolytes of a finite length[9] and thickness;[10] the effects of DNA helical structure[11] and of finite salt concentration have also been taken into account.[12] Recent single-molecule experiments on DNA translocation through artificial silicon nanopores[13] provided a direct proof of the Manning theory for B-DNA. A neutralization fraction of $\theta \approx 0.72-0.75$ was measured, almost independent of NaCl amount in a wide range from $n_0 = 0.02$ to 1 M.

Note that additional *chemical* adsorption of cations onto DNA can also occur. It depends on the counterions' chemical nature and affinity to particular sites on DNA, and not only on cation valence. This can lead to variation of θ values for cations with the same z. Also, not only θ, but also the partitioning of cations on DNA can be different (e.g., strands vs grooves adsorption, as for Mg^{2+}, Ca^{2+} vs Zn^{2+}, Mn^{2+}). These different patterns of counterions are known to affect DNA−DNA electrostatic forces. In what follows, we neglect these biochemical differences in interactions of DNA with cations and use well-established values of θ considering the DNA−DNA forces.

The forces acting between parallel DNAs are purely repulsive in solution of monovalent salts[14] and become attractive in the presence of some divalent, many trivalent, and tetravalent cations,[15−17,52] provoking DNA condensation into compact structures.[18] Equilibrium DNA−DNA separations in these condensates are ≈28−30 Å, indicating some short-ranged DNA−DNA attractive forces. This attraction is quantitatively described by the theory of electrostatic interactions of DNA duplexes, developed on the basis of the Poisson−Boltzmann equation.[19] For two closely positioned parallel or slightly interwound helically ideal DNA helices, the theory predicts also that the strength of intermolecular interactions depends on the longitudinal shift or, equivalently, on the mutual azimuthal orientation of juxtaposed DNAs.

Treatment of electrostatic interactions in *superhelical DNA plies* with arbitrary diameter and opening angles is a complicated mathematical problem. There were some suggestions in the literature for its theoretical description,[20] but the complete theory of fluctuating superhelices made of double-helically charged DNAs is still missing.

III. Ideal DNA Molecules: Intermolecular Interactions and Frictional Forces

Let us consider the forces required to slide two *ideal* closely juxtaposed parallel DNAs over each other, provided the DNA−DNA separation $2R$ is kept fixed and no DNA torsional deformations occur. The energy of electrostatic interaction of parallel double-spiral charged macromolecules has been obtained recently as an exact solution of the linear Poisson−Boltzmann theory.[21] The spirals are formed by DNA phosphate charges and cations adsorbed in DNA grooves, both treated as thin

helical continuous spirals (modifications for discrete pointlike charges have also been published).

The energy of interaction of two torsionally rigid helices of length L shifted mutually along the axis by distance δz is

$$E_{\text{int}}(R, \delta z) \approx L[a_0(R) - a_1(R) \cos(2\pi\delta z/H)]$$

where the coefficients are[22]

$$a_0(R) = \frac{8\pi^2\bar{\sigma}^2a^2}{\varepsilon}\left[\frac{(1-\theta)^2K_0(\kappa_D(2R))}{[\kappa_D a K_1(\kappa_D a)]^2} - \sum_{n,m=-\infty}^{\infty}\frac{\tilde{f}(n,\theta,f)^2K_{n-m}{}^2(\kappa_n(2R))I_m{}'(\kappa_n a)}{[\kappa_n a K_n{}'(\kappa_n a)]^2K_m{}'(\kappa_n a)}\right],$$

$$a_1(R) = \frac{16\pi^2\bar{\sigma}^2a^2}{\varepsilon}\frac{\tilde{f}(1,\theta,f)^2K_0(\kappa_1(2R))}{[\kappa_1 a K_1{}'(\kappa_1 a)]^2}$$

Here parameter f describes the partitioning of cations on DNA (at $f = 0$ all cations are adsorbed in the middle of the major groove, at $f = 1$ all are located in the minor groove; no cations are bound to DNA strands here), $\tilde{f}(n,\theta,f) = f\theta + (-1)^n(1-f)\theta - \cos(n\tilde{\phi}_s)$, $\tilde{\phi}_s \approx 0.4\pi$ is the azimuthal half-width of DNA minor groove, $\kappa_n{}^2 = \kappa_D{}^2 + (2\pi n/H)^2$ are the modified screening parameters, $1/\kappa_D = 1/(8\pi l_B n_0)^{1/2}$ is the Debye screening length, $\bar{\sigma}$ is the bare surface charge density of DNA phosphates, that is $\approx -e_0$ per 100 Å^2 on DNA surface, $a \approx 9$ Å is DNA radius, and $K_n(x)$, $I_n(x)$, $K_n{}'(x)$, and $I_n{}'(x)$ are the modified Bessel functions of order n and their derivatives.

The first term in a_0 describes the energy density of Debye−Hückel repulsion of uniformly charged rods

$$a_0{}^{\text{DH}}(R) \approx \frac{k_BT}{\text{Å}}[2.9(1-\theta)^2]\frac{(1/7)^2}{\kappa_D{}^2}\frac{K_0(\kappa_D(2R))}{K_1(\kappa_D a)^2}$$

and decays nearly exponentially with decay length $1/\kappa_D$. Repulsive DNA−DNA forces in solutions of monovalent salts can be approximated by this term.

The second term in a_0 describes the repulsive image forces acting between DNAs. DNA charged spirals are considered in the theory with a low dielectric cylindrical core. Then, the charges on one DNA generate image charges inside the core of the neighboring molecule. The image charge repulsion is important at small R, being shielded with a shorter screening length than direct rod−rod repulsion. This term provides strong repulsion for separations of 2−5 Å prior to surface−surface contact of DNAs.

The first harmonic of the direct helix−helix electrostatic interactions is described by a_1. This term accounts for cations' partitioning on DNA surface as well as for DNA double helical structure. It is screened with screening length $1/[\kappa_D{}^2 + (2\pi/H)^2]^{1/2}$ and is responsible in the theory for attraction at 28−30 Å between DNA axes.[23,24] The attraction occurs due to electrostatic zipper effect along the DNA−DNA contact. That is, negative charges on one DNA can be positioned in perfect register with positive charges of counterions adsorbed in grooves of the neighboring DNA. Attractive forces generated by interaction of two spirals can overcome the direct rod−rod and image-force repulsions only for well-neutralized DNAs (at $\theta \geq 0.7$−0.8), at high occupations of DNA major groove by cations (small f values), and in a finite range of screening lengths; see Figure 3.

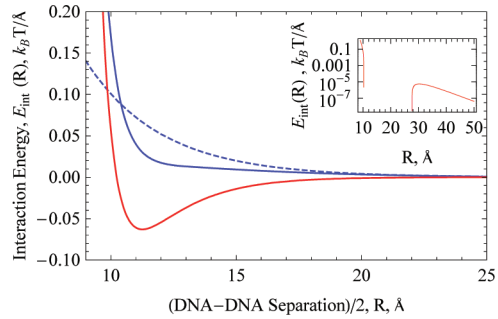

Figure 3. Energy density of electrostatic interactions of two parallel B-DNA duplexes, $E_{\text{int}}(R,0) = a_0 - a_1$, plotted for purely repulsive forces (solid blue curve at $\theta = 0.65$) and for repulsive−attractive−repulsive forces (red curve at $\theta = 0.9$). DNA−DNA attraction exists when the force $F_{\text{int}}(R) = -\partial E_{\text{int}}(R)/\partial R$ is negative. Debye−Hückel repulsion $a_0{}^{\text{DH}}(R)$ is shown as the dotted curve, plotted for $\theta = 0.65$. Other parameters: $1/\kappa_D = 7$ Å, $f = 0.3$, meaning 30% of cations in the minor and 70% in the major DNA grooves. The inset shows the log−linear energy plot at $\theta = 0.9$ with the DNA−DNA repulsion at large R.

We neglect here the contributions of further helical harmonics, $a_{n\geq 2}$. These terms are screened with shorter lengths and have much smaller magnitudes compared to $a_{0,1}$ at typical conditions and not too close to DNA−DNA contact. The total energy of DNA−DNA interactions, $E_{\text{int}}(R,0)$, can become attractive at $2R \approx 25$−35 Å and the region of attraction extends in the R domain for smaller f and larger θ.

Note that, along with electrostatics, other DNA−DNA forces can follow the DNA helical symmetry. Among them are the steric repulsions and hydration forces (caused by overlapping of lattices of ordered waters near the DNA surface upon close approach of two DNAs). One can in principle estimate the relative contribution of steric forces performing force-measurement experiments at different salt amounts.

As to hydration forces, even in well-controlled osmotic stress studies of columnar DNA assemblies, they are not easy to separate from electrostatics. It appears that force−distance curves measured by an osmotic stress technique over the last 20 Å of surface-to-surface separations prior to the contact are very similar in force magnitude and decay length for lipid membranes,[25] collagen triple helices,[26] and DNA duplexes.[27−29] In the first two systems, the hydration forces were claimed to dominate the interactions. For DNAs, however, a substantial remaining negative charge, a pronounced phosphates−cations charge alternation along the axis, and strong cation specificity of interactions indicate a sizable contribution of electrostatic interactions, possibly, in addition to hydration forces.

We use the interaction energy of parallel DNAs $E_{\text{int}}(\delta z)$ to approximate the electrostatic strand−groove register along DNA−DNA contact in ideally helical DNA superply. We do not account here for differences in interaction of left- vs right-handed plies. We also suppose that charge distribution on DNAs does not change upon DNA pulling, although the effect of mutual interactions on redistribution of adsorbed cations on closely juxtaposed DNAs can be quite substantial.[30]

The cos-like DNA−DNA interlocking defines a δz-dependent frictional force

$$F_{\text{fr,rigid,ideal}}(\delta z) = -\frac{\partial E_{int}(\delta z)}{\partial \delta z} = -La_1\frac{2\pi}{H}\sin\frac{2\pi\delta z}{H}$$

emerging upon pulling one DNA over another. This force has periodic modulations with period of DNA pitch H being responsible for the removal of the system from energy minima with the strongest DNA−DNA attraction. Stronger force modulations are expected to occur in solutions of multivalent cations that cause pronounced alternation of charges along the DNA axis (smaller f and larger θ values) and thus result in larger values of $a_1(R)$. The maximal, *static friction force* required[31,32] to overcome the potential barriers of cos-like DNA−DNA interactions at low DNA drag velocities

$$F^{\max}_{\mathrm{fr,rigid,ideal}} = \max[F_{\mathrm{fr}}]_{\delta z} = 2\pi a_1 L/H \qquad (1)$$

scales linearly with DNA length L (neglecting end effects for long molecules). For conditions favoring DNA−DNA attraction, the red curve in Figure 3, for a ply with $N = L/H$ DNA turns, $F^{\max}_{\mathrm{fr,rigid,ideal}} \approx N(0.1k_BT/\text{Å})$ at $2R = 30$ Å and $\approx N(0.009k_BT/\text{Å})$ at $2R = 40$ Å, with $k_BT/\text{Å} \approx 41$ pN. Thus, even for unrealistically tight helically ideal DNA plies with $2R = 40$ Å and at the conditions of strong DNA−DNA attraction, one cannot expect the static friction force required for DNA−DNA mutual sliding to exceed ~0.4 pN per DNA pitch.

Note that we neglect here the effects of thermal fluctuations assuming perfectly regular DNA superhelices. This static model is applicable only to tight plies, with elastic energy being much larger than entropic and confinement free energy contributions.[33] Such structures can only emerge at large stretching forces F_w in the dual optical trap apparatus. For supercoiled DNAs, when the ply radii can exceed 100 Å, the effects of thermal fluctuations are important.[34]

IV. Nonideal DNA Molecules: DNA−DNA Interactions and Electrostatic Friction

The interaction of DNAs with realistic base pair sequences differs dramatically from that of ideally helical "model" homopolymer DNAs considered above. The reason is the sequence-specific variations of DNA bp parameters, in particular of DNA bp twist angles $\langle\Omega\rangle + \delta\Omega$,[35] that have been incorporated into DNA−DNA interaction theory for both torsionally rigid[36] and torsionally flexible DNAs.

The interaction energy of two parallel torsionally rigid DNAs of length L aligned azimuthally at $z = 0$ in the same $a_{0,1}$ approximation is

$$E_{\mathrm{int}}(R) = \int_0^L [a_0(R) - a_1(R)\cos\delta\phi(z)]\,\mathrm{d}z$$

It depends on the local twist angle difference of two DNAs

$$\delta\phi(z) = \frac{1}{h}\int_0^z \delta\Omega(z)\,\mathrm{d}z$$

Here, $\delta\Omega(z)$ describes sequence-specific variations of DNA twist angles, delta-correlated for randomly sequenced DNAs, $\langle\delta\Omega(z')\,\delta\Omega(z'')\rangle = 2\Delta\Omega^2 h\delta(z'-z'')$, where $\Delta\Omega \approx 3-6°$ is the deviation of twist angles from the average value of $\langle\Omega\rangle \approx 34-36°$ for B-DNA and $h \approx H/10$ is DNA rise per base pair. The interaction energy averaged over realizations of the random field is $\langle E_{\mathrm{int}}(R)\rangle_\Omega = a_0 L - a_1\lambda_c(1 - e^{-L/\lambda_c})$. Here, the helical coherence length of twist angle fluctuations is $\lambda_c = h/\Delta\Omega^2 = 300-700$ Å for DNAs in dense assemblies and hydrated fibers.[37] Small local nonidealities of DNA helical structure caused by quasi-random walks of DNA twist angles $\delta\Omega(z)$ accumulate for DNAs considerably longer than λ_c. This *distorts* the DNA−DNA strand−groove electrostatic register and leads to reduction of zipper-like attractive energy. The helix−helix attraction can exist only for short DNA fragments, while the fragments much longer than λ_c interact nearly as uniformly charged cylinders.

The strength of frictional forces for torsionally rigid *randomly sequenced* DNAs pulled over each other is also expected to lose the proportionality to DNA length. If a DNA fragment of length L is aligned azimuthally at $z = 0$ with a long fragment of random base pairs DNA, the *average* friction force to pull the first DNA fragment is

$$\langle F_{\mathrm{fr,rigid,random}}(\delta z)\rangle \approx -a_1(1 - e^{-L/\lambda_c})e^{-\delta z/\lambda_c} \qquad (2)$$

because in this case

$$h\delta\phi(z) = \int_0^{\delta z}\delta\Omega\,\mathrm{d}z + \int_0^{z}\delta\Omega\,\mathrm{d}z$$

in the expression for $E_{\mathrm{int}}(R)$. For pulling distances δz shorter than $\sim\lambda_c$ there is some finite magnitude of frictional forces due to still existing strand−groove DNA−DNA register. As δz exceed the helical coherence length, the frictional force decays exponentially, indicating a complete decorrelation of helical charge patterns on two DNAs. DNAs interact in this regime as two uniformly charged rods and thus *have no* electrostatic friction for sliding. This is in agreement with predictions of the general theory about zero static friction between completely *incommensurate* large charged surfaces.[38]

We predict that torsionally rigid DNA helices with all base pairs identical and rigid DNAs with randomly sequenced base pairs will have *different* friction behaviors. In the first case, the difference of azimuthal angles along DNAs is zero and the molecules interact as ideal helices. Upon pulling, DNAs reveal static friction forces that grow with DNA length L. For random rigid DNAs, the frictional forces *averaged* over many realizations lose this periodic dependence on δz, the force reaches an L-independent plateau for long helices, and the force decays exponentially with the pulling distance.

For DNAs with realistic values of torsional rigidity constant, $C = k_BTl_{tw} \approx 3 \times 10^{-19}$ erg·cm, or twist persistence length of $l_{tw} \approx 750$ Å, the DNA−DNA attraction can exist even for randomly sequenced DNA fragments. This is due to substantial torsional deformations of DNA backbone enforced by intermolecular interactions that favor the perfect strand−groove DNA−DNA register. The general expressions for the interaction energy of finite-length fragments are quite cumbersome. In the limit of torsionally soft and long DNAs, however, when the major part of sequence-specific DNA twist angle variations is relaxed via DNA torsional adjustment, DNA−DNA interaction energy is again proportional to DNA length. The energy is higher than that for ideal DNAs by the cost of torsional DNA deformations toward the ideal double helix. The interaction energy in this limit of $\lambda_t \ll \lambda_c$, $L \gg \lambda_c$, is[39]

$$E_{\mathrm{int}}(R,\delta z) \approx L\left[a_0 - a_1\left(1 - \frac{\lambda_t}{4\lambda_c}\left(1 + \cos\frac{2\pi\delta z}{H}\right)\right)\right]$$

where the DNA torsional adaptation length is $\lambda_t(R) = [C/2a_1(R)]^{1/2}$. Periodic modulation of frictional forces upon

slow sliding of torsionally soft DNA-like helices is only a small fraction $\lambda_t/4\lambda_c$ from that of ideal rigid helices

$$F^{\max}_{\mathrm{fr,soft,random}} = \frac{\lambda_t}{4\lambda_c} a_1 L \frac{2\pi}{H} \quad (3)$$

Equations 1, 2, and 3 for static friction are the main results of the paper.

V. Discussion

We have discussed the magnitude of frictional forces acting between DNA molecules in the model of ideally helical duplexes, torsionally rigid randomly sequenced helices, and DNA fragments with torsionally soft backbones. Real DNAs with random sequences are in between the last two limiting cases, when frictional forces are expected to be δz-dependent and also involve DNA torsional adjustments. The detailed analysis of this case can be performed in the future, but prior to construction of a complicated model the limiting cases can be checked experimentally.

The existence of substantial frictional forces requires large a_1 values corresponding to conditions of DNA−DNA attraction. Large a_1 values exist for θ values close to unity and small f values that can be realized by addition of multivalent cations to simple salt buffers of DNA braids. This should result in formation of tight, strongly condensed DNA plies. Thus, upon addition of multivalent cations the ply radius decreases, the ply stretches, and end stretching forces applied to the beads should *decrease*. This effect of cation-induced ply shrinkage, together with dragging of one DNA in superhelical plies, can be measured in optical tweezers experiments.

The estimates obtained are valid for static friction, whereas upon faster retrieval of DNAs the kinetic friction regime can be realized. The latter is typically characterized by smaller friction coefficients and can be influenced by hydrodynamic interactions between the rubbing DNA molecules.

We used several simplifying assumptions in the estimates above. DNAs in the ply are kept in a close proximity by end forces and mechanical torques applied. Still, particularly for loose plies, local *deformations* of DNA plectonemic structure can occur (e.g., ply swelling, local DNA bending). These distortions can allow DNAs to overcome easily the electrostatic potential barriers that overlap upon DNA pulling. These elasticity effects should reduce the frictional forces; their magnitude is, however, not clear. Note also that DNA−DNA molecular friction of a nonelectrostatic nature can occur along the contact as well, e.g., due to steric clashes of grooves of moving DNAs. This effect is also not considered here.

Ideal superhelices were considered; realistic DNA plies are, however, never ideal. Thermal fluctuations are expected to distort DNA−DNA register on the nanoscale and weaken helix-specific interactions. In dual optical tweezers experiments on DNA plies under external tension by Wuite, the friction force measured remained well below 1 pN. To observe DNA−DNA electrostatic friction by this setup, ply diameters of ≤30−40 Å should be maintained because the helix-specific DNA−DNA interactions decay rapidly with separation. Such extremely tight plies need *large* external forces and torques applied to the DNAs[40−42] by the end beads. To resolve the force modulations that are caused by DNA intrinsic helicity by this method, a spatial resolution of at least $H/2$ is required. The current resolution is nearly 1 order of magnitude worse, which does not allow the extraction of force modulations for two sliding DNAs on nm length scale.

Above, we have assumed that friction in DNA superhelical plies can be captured via interactions of *parallel* DNAs. It can be valid for static DNA plies with superhelical pitch P much larger than DNA pitch H. When these two are of the same order, more complicated expressions for DNA−DNA electrostatic interactions are required. This problem involves *chiral* DNA−DNA electrostatic interactions[43,44] and we do not treat it here.

For plies made of model *right-handed net-neutral* helices in nonpolar salt-free environment, the *left-handed* supercoils were predicted by the theory; see section 5H of ref 45. Such spirality allows a better alignment of positive strands of charges on one helix with negative strands on the other, thus lowering the interaction energy.[46] A drawback of this model is that net-neutral helices attract each other at all separations having the $R = 0$ state as the energy minimum, and thus no prediction is possible for the *optimal ply thickness*.

For DNA double-stranded helices, the influence of noncompensated DNA charge, the image forces disfavoring thin superhelical DNA plies, and screening by electrolyte onto the optimal ply pitch and diameter has to be considered. It is beyond the scope of classical models of DNA supercoils[47−50] and is a problem for a separate study. In this context, it would be interesting in particular to analyze how strongly chiral DNA−DNA interactions affect the opening angles α of closed negatively supercoiled DNA plasmids. The latter were measured to be $\alpha \approx 55°$, nearly independent of the degree of DNA supercoiling.[51]

VI. Conclusions

Dragging one DNA over another one in tight DNA superhelical plies in dual optical tweezers apparatus seems to be a suitable tool to probe the existence of DNA−DNA electrostatic frictional forces on the nanoscale. This paper is a first attempt to estimate theoretically the magnitude of possible DNA−DNA friction. The friction forces of ideal DNAs are expected to grow with the number of DNA turns in the ply because DNA−DNA interaction energy scales linearly with ply length. A *stick−slip*-like motion on scale of 3.4 nm is expected to occur for *slow* pulling of two *ideal* DNAs over each other. It originates from *charge interlocking* of strands and grooves of DNAs in close contact, with 5−10 Å between DNA surfaces. These interlocks are expected to be most pronounced for DNAs in solution of multivalent cations. Ideal DNA homopolymers should reveal *higher* static friction forces due to fully commensurate potential variations, compared to randomly sequenced rigid DNA fragments where interlocks become decorrelated and friction forces depend on the pulling distance. Large ply stretching forces and tight plies as well as slow DNA drag velocities are required to detect DNA−DNA friction forces in protein-free buffers.

Acknowledgment. I acknowledge support from the Deutsche Forschungsgemeinschaft, Grant CH 707/2-1. I thank the referees for insightful comments on an earlier version of the paper.

References and Notes

(1) Noom, M. C.; et al. *Nat. Methods* **2007**, *4*, 1031.
(2) Dame, R. T.; et al. *Nature* **2006**, *444*, 387.
(3) Charvin, G.; et al. *Annu. Rev. Biophys. Biomol. Struct.* **2005**, *34*, 201.
(4) Charvin, G.; et al. *Biophys. J.* **2005**, *88*, 4124.
(5) Marko, J. F. *Phys. Rev. E* **1997**, *55*, 1758.
(6) Cherstvy, A. G.; Winkler, R. G. *J. Chem. Phys.* **2004**, *120*, 9394.
(7) Manning, G. S. *Q. Rev. Biophys.* **1978**, *11*, 179.
(8) Manning, G. S. *J. Phys. Chem. B* **2007**, *111*, 8554.

(9) Castelnovo, M.; Sens, P.; Joanny, J.-F. *Eur. Phys. J. E* **2000**, *1*, 115.
(10) Schurr, J. M.; Fujimoto, B. S. *Biophys. Chem.* **2002**, *101−102*, 425.
(11) Manning, G. S. *Macromolecules* **2001**, *34*, 4650.
(12) Muthukumar, M. *J. Chem. Phys.* **2004**, *120*, 9343.
(13) Keyser, U. F.; et al. *Nat. Phys.* **2006**, *2*, 473.
(14) Rau, D. C.; et al. *Proc. Natl. Acad. Sci. U.S.A.* **1984**, *81*, 2621.
(15) Leikin, S.; Rau, D. C.; Parsegian, V. A. *Phys. Rev. A* **1991**, *44*, 5272.
(16) Rau, D. C.; Parsegian, V. A. *Biophys. J.* **1992**, *61*, 260.
(17) Guldbrand, L.; Nilsson, L.; Nordenskiöld, L. *J. Chem. Phys.* **1986**, *85*, 6686.
(18) Bloomfield, V. A. *Curr. Opin. Struct. Biol.* **1996**, *6*, 334.
(19) Kornyshev, A. A.; Leikin, S. *J. Chem. Phys.* **1997**, *107*, 3656.
(20) Lee, D. J.; et al. Work in preparation.
(21) Kornyshev, A. A.; Leikin, S. *Phys. Rev. Lett.* **1999**, *82*, 4138.
(22) Cherstvy, A. G.; Kornyshev, A. A. *J. Phys. Chem. B* **2005**, *109*, 13024.
(23) Cherstvy, A. G. *J. Phys.: Condens. Matter* **2005**, *17*, 1363.
(24) Cherstvy, A. G. *J. Phys. Chem. B* **2007**, *111*, 7914.
(25) Rand, R. P.; Parsegian, V. A. *Biochim. Biophys. Acta* **1989**, *988*, 351.
(26) Leikin, S.; Rau, D. C.; Parsegian, V. A. *Nat. Struct. Biol.* **1995**, *2*, 205.
(27) Leikin, S.; et al. *Annu. Rev. Phys. Chem.* **1993**, *44*, 369.
(28) Yang, J.; Rau, D. C. *Biophys. J.* **2007**, *89*, 1932.
(29) Todd, B. A.; et al. *Biophys. J.* **2008**, *94*, 4775.
(30) Cherstvy, A. G.; Kornyshev, A. A.; Leikin, S. *J. Phys. Chem. B* **2002**, *106*, 13362.
(31) Rozman, M. G.; et al. *Phys. Rev. Lett.* **1996**, *77*, 683.
(32) Panyukov, S.; Rabin, Y. *Phys. Rev. E* **1997**, *56*, 7053.
(33) Odijk, T. *Macromolecules* **1983**, *16*, 1340.
(34) Purohit, P. K. *J. Mech. Phys. Solids* **2008**, *56*, 1715.
(35) Olson, W. K.; et al. *Proc. Natl. Acad. Sci. U.S.A.* **1998**, *95*, 11163.
(36) Kornyshev, A. A.; Leikin, S. *Phys. Rev. Lett.* **2001**, *86*, 3666.
(37) Wynveen, A.; et al. *Nucleic Acids Res.* **2008**, *36*, 5540.
(38) Muser, M. H.; et al. *Adv. Chem. Phys.* **2003**, *126*, 187.
(39) Cherstvy, A. G.; Kornyshev, A. A.; Leikin, S. *J. Phys. Chem. B* **2004**, *108*, 6508.
(40) Yabuta, T. *Bull. JSME* **1984**, *27*, 231.
(41) Coyne, J. *IEEE J. Oceanic Eng.* **1990**, *15*, 72.
(42) Starostin, E. L. *Meccanica* **1996**, *31*, 235.
(43) Kornyshev, A. A.; Leikin, S. *Phys. Rev. E* **2000**, *62*, 2576.
(44) Kornyshev, A. A.; Leikin, S.; Malinin, S. V. *Eur. Phys. J. E* **2002**, *7*, 83.
(45) Kornyshev, A. A.; Lee, D. J.; Leikin, S.; Wynveen, A. *Rev. Mod. Phys.* **2007**, *79*, 943.
(46) Cherstvy, A. G. *J. Phys. Chem. B* **2008**, *112*, 12585.
(47) Marko, J. F.; Siggia, E. D. *Phys. Rev. E* **1995**, *52*, 2912.
(48) Ubbink, J.; Odijk, T. *Biophys. J.* **1999**, *76*, 2502.
(49) Clauvelin, N.; Audoly, B.; Neukirch, S. *Macromolecules* **2008**, *41*, 4479.
(50) Vologodskii, A. V.; Marko, J. F. *Biophys. J.* **1997**, *73*, 123.
(51) Boles, T. C.; et al. *J. Mol. Biol.* **1990**, *213*, 931.
(52) Pietronave, S.; Arcesi, L.; D'Arrigo, C.; Perico, A. *J. Phys. Chem. B,* **2008**, *112*, 15991.

JP810473M